MOLECULAR AND CELLULAR BIOLOGY, June 1991, p. 3203–3216
0270-7306/91/063203-14$02.00/0

Vol. 11, No. 6

GCD2, a Translational Repressor of the *GCN4* Gene, Has a General Function in the Initiation of Protein Synthesis in *Saccharomyces cerevisiae*

MARCO FOIANI, A. MARK CIGAN, CHRISTOPHER J. PADDON,† SATOSHI HARASHIMA,‡ AND ALAN G. HINNEBUSCH*

Section on Molecular Genetics of Lower Eukaryotes, National Institute of Child Health and Human Development, Bethesda, Maryland 20892

Received 18 January 1991/Accepted 27 March 1991

The GCD2 protein is a translational repressor of *GCN4*, the transcriptional activator of multiple amino acid biosynthetic genes in *Saccharomyces cerevisiae*. We present evidence that GCD2 has a general function in the initiation of protein synthesis in addition to its gene-specific role in translational control of *GCN4* expression. Two temperature-sensitive lethal *gcd2* mutations result in sensitivity to inhibitors of protein synthesis at the permissive temperature, and the *gcd2-503* mutation leads to reduced incorporation of labeled leucine into total protein following a shift to the restrictive temperature of 36°C. The *gcd2-503* mutation also results in polysome runoff, accumulation of inactive 80S ribosomal couples, and accumulation of at least one of the subunits of the general translation initiation factor 2 (eIF-2α) in 43S-48S particles following a shift to the restrictive temperature. The *gcd2-502* mutation causes accumulation of 40S subunits in polysomes, known as halfmers, that are indicative of reduced 40S-60S subunit joining at the initiation codon. These phenotypes suggest that GCD2 functions in the translation initiation pathway at a step following the binding of eIF-2 · GTP · Met-tRNA$_i^{Met}$ to 40S ribosomal subunits. Consistent with this hypothesis, we found that inhibiting 40S-60S subunit joining by deleting one copy (*RPL16B*) of the duplicated gene encoding the 60S ribosomal protein L16 qualitatively mimics the phenotype of *gcd2* mutations in causing derepression of *GCN4* expression under nonstarvation conditions. However, deletion of *RPL16B* also prevents efficient derepression of *GCN4* under starvation conditions, indicating that lowering the concentration of 60S subunits and reducing GCD2 function affect translation initiation at *GCN4* in different ways. This distinction is in accord with a recently proposed model for *GCN4* translational control in which ribosomal reinitiation at short upstream open reading frames in the leader of *GCN4* mRNA is suppressed under amino acid starvation conditions to allow for increased reinitiation at the *GCN4* start codon.

In the yeast *Saccharomyces cerevisiae*, starvation for an amino acid or reduced aminoacyl-tRNA synthetase function leads to increased transcription of over 30 genes encoding amino acid biosynthetic enzymes in 11 different pathways (general amino acid control). This cross-pathway response occurs because synthesis of GCN4 protein, a transcriptional activator of these genes, increases under conditions of amino acid starvation (reviewed in reference 25). *GCN4* expression is regulated by amino acid availability at the translational level by a mechanism involving four short upstream open reading frames (uORFs) in the leader of *GCN4* mRNA. A subset of these uORFs blocks the flow of scanning ribosomes to the *GCN4* start codon under nonstarvation conditions. This translational repression by the uORFs is dependent on *trans*-acting negative regulators of *GCN4* expression encoded by *GCD* genes. Positive regulators encoded by *GCN1*, *GCN2*, and *GCN3* stimulate *GCN4* translation in amino acid-starved cells. GCN1, GCN2, and GCN3 appear to act by antagonizing GCD factors because *gcd* mutations overcome the requirement for these positive effectors for derepression of *GCN4* (25). Recently, mutations have been isolated in the structural genes for the alpha and beta subunits of the general translation initiation factor 2 (eIF-2) that derepress *GCN4* expression in the same manner described previously for *gcd* mutations (54). This is one of several observations suggesting that translation of *GCN4* mRNA is stimulated under conditions in which general translation initiation is reduced (52).

In addition to causing derepression of *GCN4*, all known *gcd* mutations lead to slow growth or temperature-sensitive growth under nonstarvation conditions. Furthermore, deletions of *GCD1* and *GCD2* are unconditionally lethal (25). Because *GCN4* is dispensable under nonstarvation conditions, these findings indicate that GCD factors have an essential function in addition to their roles in general amino acid control. Given their involvement in regulating *GCN4* translation, a function in general protein synthesis has been considered a likely possibility. In accord with this notion, the temperature-sensitive lethal *gcd1-101* mutation leads to lower rates of incorporation of radiolabeled amino acids (50, 55) and reduced amounts of a translation initiation intermediate containing charged initiator tRNA (52) following a shift to the nonpermissive temperature. In this report, we examine the role of the GCD2 protein in the process of translation initiation.

Considerable genetic evidence exists that the GCN3 protein contributes to the essential functions of GCD1 and GCD2 in addition to its role as a positive regulator of *GCN4* translation. For example, certain mutations in *GCD2* (*gcd2-502* and *gcd2-503*) were isolated that overcome the low-level

* Corresponding author.
† Present address: Genetics Department, Glaxo Group Research Limited, Greenford, Middlesex, UB6 OHE, England.
‡ Present address: Department of Fermentation Technology, Faculty of Engineering, Osaka University, Osaka 565, Japan.

GCN4 expression associated with a *gcn3-101* mutation, leading to a constitutively derepressed (Gcd^-) phenotype and temperature-sensitive growth under nonstarvation conditions (20, 41). Surprisingly, wild-type *GCN3* restores both the essential and the negative regulatory functions of *GCD2* impaired in these *gcd2* mutants. Similar results were obtained for a group of *gcd1* mutations isolated as suppressors of *gcn3-101* (19), and the temperature-sensitive *gcd1-101* mutation is unconditionally lethal in combination with a *gcn3* deletion (17). In addition, there is significant amino acid sequence similarity between GCN3 and the carboxyl-terminal half of GCD2, supporting the idea that these two proteins have closely related functions (40). Indeed, recent biochemical studies indicate that GCD1, GCD2, and GCN3 exist in the same high-molecular-weight protein complex (6a). The latter finding suggests that wild-type GCN3 protein overcomes the mutant phenotypes of the aforementioned *gcd1* and *gcd2* mutations by stabilizing the thermolabile *gcd*-encoded proteins present in the same complex (19). In wild-type cells under starvation conditions, GCN3 is thought to mediate the effects of GCN1 and GCN2 in reducing the functions of GCD proteins with which it associates as the means of stimulating *GCN4* translation.

Genetic interactions similar to those just described involving *GCD1*, *GCD2*, and *GCN3* have also been noted between *GCN3* and *SUI2*, the structural gene for the alpha subunit of eIF-2. The *sui2-1* mutation leads to constitutive derepression of *GCN4* expression (Gcd^- phenotype) and temperature-sensitive growth under nonstarvation conditions and is unconditionally lethal when combined with a deletion of *GCN3* (54). This synthetic lethality suggests that GCN3, and by extension GCD1 and GCD2, interact with eIF-2 in carrying out an essential function in translation initiation. The best-studied function of eIF-2 involves the formation of a ternary complex containing GTP and Met-$tRNA_i^{Met}$ and binding of this complex to a 43S species consisting of the small ribosomal subunit and additional initiation factors. The 43S preinitiation complex thus formed binds to mRNA and scans the mRNA leader for the AUG start codon, whereupon GTP is hydrolyzed and eIF-2 is released from the ribosome (36). Thus, eIF-2 is directly involved in several reactions of the initiation pathway, any one of which might involve GCD1, GCD2, and GCN3.

In this report we describe the effects of the *gcd2-502* and *gcd2-503* mutations on the process of general translation initiation. The results provide strong support for the notion that GCD2 protein is an essential component of the initiation machinery and that the dispensable positive regulator GCN3 contributes to this general function in protein synthesis. Our findings suggest that both *gcd2* mutants are impaired in a late step in the translation initiation pathway, following the formation of preinitiation complexes containing eIF-2 and the binding of these complexes to small ribosomal subunits to form 43S intermediates. In particular, the *gcd2-502* mutant appears to be affected either in scanning, AUG start codon recognition during the scanning process, or the subsequent reactions required for 40S-60S subunit joining at the AUG codon. Accordingly, we reasoned that reducing 40S-60S subunit joining by lowering the concentration of 60S subunits by deleting one copy (*RPL16B*) of the duplicated gene encoding ribosomal protein L16 should resemble *gcd2* mutations in causing derepression of *GCN4* expression under nonstarvation conditions. Our results confirm this expectation, supporting the notion that decreasing the efficiency of a late step in the general initiation pathway is responsible for increased translation at *GCN4*. However, the mutations in *GCD2* and *RPL16B* differ significantly in their quantitative effects on *GCN4* expression, and this difference has important implications for the mechanism of *GCN4* translational control.

MATERIALS AND METHODS

Plasmids. Plasmid Ep321 contains *GCN3* on a 4.0-kb *Eco*RI-*Bam*HI fragment isolated from Ep69 (17) and inserted between the *Eco*RI and *Bam*HI sites of YIp5 (49). Plasmid pM214 was constructed by inserting the 2.5-kb *Kpn*I fragment from p611 (16) containing the *URA3* gene into the *Kpn*I site in the *GCN4* coding region of plasmid pAH38 (24). Plasmid pMF12 contains *GCD2* on a 2.6-kb *Cla*I-*Eag*I fragment isolated from pCP46 (41) and inserted between the *Cla*I and *Eag*I sites of YIp5. Plasmid pCP57 contains the 2.6-kb *Sal*I-*Eag*I fragment from pCP46 inserted between the *Sal*I and *Eag*I sites of YEp24 (5). Plasmids p180, p226, and p227 containing *GCN4-lacZ* fusions were already described (37). Plasmid pGOBLEU containing the *rp51a*::*LEU2* allele was kindly provided by Nadja Abovich of Brandeis University. Plasmids pl16bΔLEU and pY1rA12, containing the *rpl16b*::*LEU2* and yeast ribosomal DNA repeat unit, respectively, were kindly provided by John L. Woolford of Carnegie-Mellon University.

Yeast strains. Table 1 lists the yeast strains used. The wild-type *GCD2* strains H1453, H1459, and H1457 were constructed from H952, H625, and H630, respectively, by gene replacement using plasmid pMF12 containing the *GCD2* gene. The plasmid was digested at the *Bgl*II site upstream of *GCD2* (40) and used to transform H952, H625, and H630 to Ura^+ and temperature resistance (Tsm^+) (27). Beginning with Ura^+ Tsm^+ transformants, we selected for loss of the plasmid-borne *URA3* gene by the 5-fluoro-orotic acid-positive selection procedure (4). Ura^- colonies were purified and screened for the temperature-resistant phenotype indicative of replacement of a *gcd2* allele with wild-type *GCD2*. In the case of H1459 and H1457, the strains showed the expected sensitivity to 3-aminotrazole (3-AT; an inhibitor of histidine biosynthesis) associated with *gcn3-101* (25). The wild-type *GCN3* strains H1462 and H1458 were constructed from H625 and H630, respectively, by gene replacement using plasmid Ep321 containing the *GCN3* gene. The plasmid was digested at the *Hin*dIII site upstream of *GCN3* (17) and used to transform H625 and H630 to Ura^+. Ura^- colonies were isolated as described above and screened for resistance to 3-AT and temperature resistance, indicative of replacement of *gcn3-101* with wild-type *GCN3*. H1456 was a Ura^- derivative showing the same phenotype as the parental strain H630 and thus had retained the *gcn3-101* allele. *RPL16B* in H1402, H1333, and H1511 strains was replaced with the *rpl16b*::*LEU2* deletion/insertion allele, forming strains H1532, H1533, and H1675, respectively, by one-step gene replacement using plasmid pl16bΔLEU, as previously described (47). Deletion of *RPL16B* was confirmed by DNA blot hybridization analysis (data not shown). H1550 and H1555 were meiotic segregants of a cross between H1532 and EY163 that contain the *HIS4-lacZ* fusion, the latter being identified by the formation of blue colonies on medium containing 5-bromo-4-choro-3-indolyl-β-D-galactopyranoside (X-Gal). *GCN4* in H1402 and H1532 was replaced with a *gcn4*::*URA3* deletion/insertion allele, forming strains H1652 and H1653 respectively, by one-step gene replacement using the 3.7-kb *Bst*EII-*Mlu*I fragment from pM214 to transform H1402 and H1532 to Ura^+. Deletion of *GCN4* was confirmed by DNA blot hybridization analysis (data not

TABLE 1. *S. cerevisiae* strains

Strain	Genotype	Reference or source
H4	*MATa ura3-52 leu2-3 leu2-112*	17
H64	*MATα gcn2-101 gcn3-101 gcd2-503*[a] *his1-29 ura3-52 HIS4-lacZ*	20
H96	*MATα gcn2-101 gcn3-101 hisl-29 ura3-52 HIS4-lacZ*	20
H625	*MATa gcd2-503 gcn3-101 ura3-52*	19
H630	*MATa gcd2-502 gcn3-101 ura3-52 leu2-3 leu2-112*	19
H952	*MATα gcd2-1 ura3-52 leu2-3 leu2-112*	41
H1333	*MATα inol ura3-52 leu2-3 leu2-112 HIS4-lacZ gcn2::URA3*	16
H1402	*MATα inol ura3-52 leu2-3 leu2-112 HIS4-lacZ*	16
H1453	*MATα ura3-52 leu2-3 leu2-112*	This study
H1456	*MATa gcd2-502 gcn3-101 ura3-52 leu2-3 leu2-112*	This study
H1457	*MATa gcn3-101 ura3-52 leu2-3 leu2-112*	This study
H1458	*MATa gcd2-502 ura3-52 leu2-3 leu2-112*	This study
H1459	*MATa gcn3-101 ura3-52*	This study
H1462	*MATa gcd2-503 ura3-52*	This study
H1489	*MATα inol ura3-52 leu2-3 leu2-112 HIS4-lacZ gcn3*^{c}*R104K*	16
H1511	*MATα ura3-52 trp1-63 leu2-3 leu2-112 GAL2*$^{+}$	This study
H1532	*MATα inol ura3-52 leu2-3 leu2-112 HIS4-lacZ rp116b::LEU2*	This study
H1533	*MATα inol ura3-52 leu2-3 leu2-112 HIS4-lacZ rp116b::LEU2 gcn2::URA3*	This study
H1550	*MATα inol ura3-52 leu2-3 leu2-112 HIS4-lacZ gcn3::URA3*	This study
H1555	*MATα inol ura3-52 leu2-3 leu2-112 HIS4-lacZ rp116b::LEU2 gcn3::URA3*	This study
H1652	*MATα inol ura3-52 leu2-3 leu2-112 HIS4-lacZ gcn4::URA3*	This study
H1653	*MATα inol ura3-52 leu203 leu2-112 HIS4-lacZ rp116b::LEU2 gcn4::URA3*	This study
H1654	*MATα inol ura3-52 leu2-3 leu2-112 HIS4-lacZ rp51a::LEU2*	This study
H1675	*MATα ura3-52 trp1-63 leu2-3 leu2-112 GAL2*$^{+}$ *rp116b::LEU2*	This study
EY163	*MATa ura3-52 leu2-3 leu2-112 gcn3::URA3*	E. Hannig
TP11B-4-1	*MATa adel leu2-3 leu2-112 ura3-52 prt1-1*	G. Johnston
FY14	*MATa ura3-52 trp1Δ-63*	F. Winston

[a] The *gcd2-502* and *gcd2-503* alleles were originally described as *gcd12-502* and *gcd12-503*, respectively, prior to the demonstration that *GCD12* and *GCD2* are the same gene (41).

shown). The *RP51A* gene in H1402 was replaced with a *rp51a::LEU2* deletion/insertion allele, forming strain H1654, by one-step replacement using plasmid pGOBLEU as described previously (2). The deletion of *RP51A* was confirmed by DNA blot hybridization analysis (data not shown). Strain TP11B-4-1 was kindly provided by Gerry Johnston of Dalhousie University. H1511 was derived from a genetic cross between H1402 and FY14 (the latter kindly provided by Fred Winston of Harvard Medical School). EY163 was kindly provided by Ernest Hannig of this laboratory.

Measurement of radioactive leucine incorporation into protein. *gcd2-503* strain H64 and the isogenic *GCD2* strain H96 were grown to saturation in SD medium containing the necessary supplements, diluted 1:50 into the same medium, and cultured at 23°C for 4 h to the beginning of exponential growth. [^{3}H]leucine was added to 1 μCi/ml, and after 15 min the cultures were divided in half and placed in water bath shakers at 23 or 36°C. Aliquots of the cultures were taken at 2-h intervals and assayed for A_{650}, as an estimate of cell mass, and for incorporation of radiolabeled leucine into protein as described previously (55).

Antibodies and immunoblot analysis. Rabbit antibodies against GCD2 were generated by using a TrpE-GCD2 fusion protein expressed in *Escherichia coli* from plasmid pCP50, the construction of which was previously described (40). Induction and extraction of the fusion protein were carried out exactly as described previously (30). The specificity and titer of the serum obtained was determined by immunoblot analysis of crude extracts of transformants of yeast strain H4 containing single or high-copy-number *GCD2* plasmids. Yeast crude extracts were prepared as previously described (11) except that cells were grown in SD medium lacking uracil. Samples (50 μg) of total cellular protein were separated by electrophoresis in 10% sodium dodecyl sulfate-polyacrylamide gels (SDS-PAGE) (32), transferred to nitrocellulose (51), and incubated with a blocking solution of 5% nonfat dry milk in phosphate-buffered saline (PBS) containing 0.2% Triton X-100. The filter was incubated overnight at room temperature with total serum diluted 1:500 in blocking solution. The filter was washed four times with PBS, and immunocomplexes were detected by using alkaline phosphatase-conjugated secondary antibodies (Bio-Rad). As shown in Fig. 5, the serum identified a protein in yeast crude extracts with an apparent M_r of 70,000, in good agreement with the estimated molecular weight of GCD2 (40). As expected, this protein was present in greater abundance when *GCD2* was present on the high-copy-number plasmid pCP57 (see Fig. 5); in addition, we found that *gcd2* mutations specifically reduced the steady-state level of this protein in crude extracts (data not shown). Antibodies against the alpha subunit of eIF-2 were provided by Thomas Donahue of Indiana University.

Preparation and gradient analysis of yeast polysomes and ribosomes. Yeast cultures (300 ml) were grown in YPD at 23°C to an optical density at 600 nm (OD_{600}) of 1.0. One-half of the culture was harvested by centrifugation at room temperature, resuspended in 15 ml of YPD at room temperature, added to 135 ml of YPD prewarmed to 37°C, and incubated for 30 min in a 37°C water bath shaker. The remaining half of the culture was maintained at 23°C. At the end of the incubation period, cycloheximide was added at a final concentration of 50 μg/ml, and the cultures were placed immediately in ice water. Cells were harvested and washed with 10 ml of ice-cold breaking buffer A (10 mM Tris-HCl [pH 7.4], 100 mM NaCl, 30 mM $MgCl_2$, 50 μg of cycloheximide per ml, 200 μg of heparin per ml), centrifuged at 3,600 × *g* for 5 min, and resuspended in 1 ml of breaking buffer. Glass beads were added to about one-fourth of the total

volume and vortexed 10 times for 20 s with 30-s intervals on ice. The extracts were cleared by two sequential centrifugation steps (5,000 × *g* for 5 min and 12,000 × *g* for 10 min). Twenty-five OD_{260} units of supernatant was layered on 12-ml linear 7 to 47% or 15 to 35% low-salt sucrose gradients containing 50 mM Tris-acetate (pH 7.0), 50 mM NH_4Cl, 12 mM $MgCl_2$, and 1 mM dithiothreitol and centrifuged in an SW41 rotor at 4°C at 39,000 rpm for 2.5 or 4.5 h, respectively. The gradients were scanned at 254 nm and fractionated in an ISCO gradient collector, taking 0.2- or 0.6-ml fractions. For high-salt sucrose gradients, 7 to 47% sucrose gradients were prepared with the buffer described above except containing 0.7 M NaCl. NaCl was added at 0.8 M to the different samples before they were layered on these gradients. For low-Mg^{2+} gradients, cells were harvested and washed in breaking buffer B (50 mM Tris-HCl [pH 7.4], 50 mM NaCl, 1 mM dithiothreitol), processed as described above, and centrifuged on 7 to 47% sucrose gradients prepared in breaking buffer B.

Proteins were precipitated from 0.60-ml gradient fractions by the addition of 0.2 ml of 50% trichloroacetic acid (TCA) and incubated overnight at −20°C. Proteins were pelleted in a microfuge for 15 min, washed twice with ice-cold acetone, dried under vacuum, and resuspended in 70 μl of Laemmli loading buffer (32). Samples of 35 μl were boiled for 3 min, subjected to SDS-PAGE and analyzed by immunoblotting as described above. Total RNA was precipitated from 0.2-ml gradient fractions by the addition of 0.5 ml of cold ethanol and incubated at −20°C overnight. The RNA was pelleted in a microfuge and purified as described previously (47). RNA samples were lyophilized and resuspended in 50 μl of H_2O, and 5 μl of each was fractionated by electrophoresis in a 1.2% formaldehyde-agarose gel, transferred to Gene-Screen Plus membrane (Dupont), and probed with ^{32}P-labeled pY1rA12 plasmid DNA containing the yeast ribosomal DNA repeat unit (44). Plasmid DNA was labeled by the random primer technique (12). Autoradiograms of the filters were prepared, and the amounts of radiolabeled species were measured with a scanning densitometer (Helena Laboratories Co.).

Assay of *HIS4-lacZ* and *GCN4-lacZ* fusions. β-Galactosidase assays were conducted as described previously (33) on extracts prepared from transformants grown in SD medium containing only the required supplements. For nonstarvation (repressing) conditions, saturated cultures were diluted 1:50 and harvested in mid-exponential phase after 6 h of growth. For starvation (derepressing) conditions, cultures were grown for 2 h under nonstarvation conditions and then for 6 h after 3-AT was added to 10 mM. β-Galactosidase activities were expressed as nanomoles of *o*-nitrophenyl-β-D-galactopyranoside hydrolyzed per minute per milligram of protein.

RESULTS

***gcd2* mutants are sensitive to inhibitors of translation.** To investigate whether GCD2 has a general role in translation, we began by testing *gcd2* mutants for sensitivity to cycloheximide and neomycin, both of which inhibit translation elongation in vitro. At low concentrations, cycloheximide specifically inhibits translation initiation (3, 8, 22, 42). As shown in Table 2, the *gcd2-1 GCN3* strain H952, *gcd2-502 gcn3-101* strain H1456, and *gcd2-503 gcn3-101* strain H625 are all temperature sensitive for growth on nutrient-rich medium (YPD) relative to their respective isogenic wild-type *GCD2* strains H1453, H1457, and H1459. As expected from previous findings (19), the temperature-sensitive growth

TABLE 2. Sensitivity of *gcd2* mutants to neomycin and cycloheximide

Strain	Relevant genotype	Growth[a]			
		23°C[b]	37°C[b]	Neo, 23°C[c]	Cyh, 23°C[d]
H952[e]	*gcd2-1 GCN3*	+	−	−	−
H1453[e]	*GCD2 GCN3*	+	+	+	+/−
H1456[f]	*gcd2-502 gcn3-101*	+	−	−	−
H1457[f]	*GCD2 gcn3-101*	+	+	+	−
H1458[f]	*gcd2-502 GCN3*	+	+	+	−
H625[g]	*gcd2-503 gcn3-101*	+	−	−	−
H1459[g]	*GCD2 gcn3-101*	+	+	+	+
H1462[g]	*gcd2-503 GCN3*	+	+	+	+

[a] Strains were replica printed to the indicated media and scored for growth after 2 to 3 days. +, confluent growth; +/−, weak growth; −, no visible growth.
[b] YPD medium containing no drugs.
[c] YPD medium containing neomycin at 5 mg/ml.
[d] YPD medium containing cycloheximide at 0.1 μg/ml.
[e] Isogenic strains.
[f] Isogenic strains.
[g] Isogenic strains.

associated with *gcd2-502* and *gcd2-503* was not observed in strains H1458 and H1462 that contain the wild-type allele of *GCN3*. By contrast, the temperature-sensitive phenotype of the *gcd2-1* mutation is expressed independent of the *GCN3* allele (41). The *gcd2* mutants H952, H1456, and H625 were found to be sensitive to neomycin on YPD medium at the permissive growth temperature of 23°C compared with the corresponding isogenic *GCD2* strains H1453, H1457, and H1459. Two of these mutants (H952 and H625) also showed sensitivity to a low concentration of cycloheximide on YPD medium at 23°C. (The cycloheximide sensitivity associated with the *gcd2-502* mutation in H1456 could not be assessed because the isogenic wild-type *GCD2* strain H1457 is sensitive to this drug.) For the *gcd2-502* and *gcd2-503* mutations, whose temperature-sensitive growth phenotypes are not expressed in the presence of wild-type *GCN3*, we found that the drug sensitivity associated with these mutations was also overcome by wild-type *GCN3* (compare the neomycin sensitivity of the *gcd2 gcn3-101* strains H1456 and H625 with that of the corresponding isogenic *gcd2 GCN3* strains H1458 and H1462 in Table 2). These findings are consistent with the idea that *gcd2* mutations partially impair general protein synthesis at permissive temperatures, conditions in which they lead to derepression of *GCN4* translation (20).

***gcd2-503 gcn3-101* mutants are temperature sensitive for incorporation of radioactive amino acids into protein.** We next compared the ability of isogenic *GCD2 gcn3-101* and *gcd2-503 gcn3-101* strains to incorporate radiolabeled leucine into proteins during growth at 23°C and at various times following a shift to the nonpermissive temperature. We focused on the *gcd2-503* allele in this analysis because, of the known mutations in *GCD2*, it has the most severe effect on growth at 36°C (data not shown). At 23°C, the growth rates of the *GCD2 gcn3-101* strain H96 and the *gcd2-503 gcn3-101* mutant H64 were nearly indistinguishable. After being shifted to 36°C, the *GCD2 gcn3-101* strain doubled three times in cell mass (OD_{650}) during the first 6 h of incubation, whereas the *gcd2-503 gcn3-101* mutant doubled only once during the same period of time and arrested with an unbudded cell morphology, as reported previously (19) (data not shown). At 23°C, the rates of [^3H]leucine incorporation were nearly identical between the *gcd2-503* mutant and wild-type *GCD2* strains (Fig. 1A). By contrast, the *gcd2-503* mutant showed

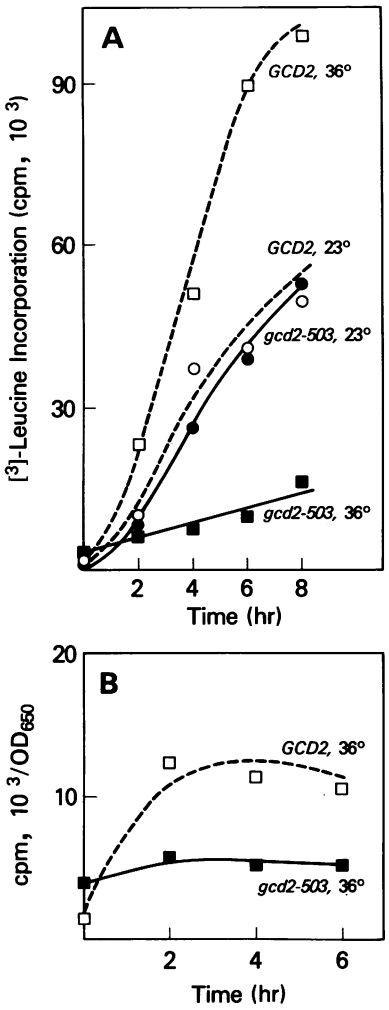

FIG. 1. (A) Incorporation of radioactive leucine into protein in *gcd2-503* and *GCD2* strains. Exponentially growing cultures of isogenic strains H64 (*gcd2-503 gcn2-101 gcn3-101*) and H96 (*GCD2 gcn2-101 gcn3-101*) were labeled with [^{3}H]leucine at 23°C, and at time zero, one-half of the culture was shifted to 36°C. Aliquots were taken at 2-h intervals to assay the amount of TCA-insoluble counts per minute, plotted here as a function of time. (B) The counts per minute of [^{3}H]leucine incorporated into protein was divided by the OD_{650} of the culture at each time point for the H96 (*GCD2*) and H64 (*gcd2-503*) cultures incubated at 36°C. (The comparable curves for the two cultures maintained at 23°C were nearly superimposable for H96 and H64.)

a much lower rate of [^{3}H]leucine incorporation within the first 2 h following the shift from 23 to 36°C (done at time zero) and throughout the period of incubation at the restrictive temperature than did the wild-type *GCD2* strain under the same conditions (Fig. 1A). After normalizing for the OD_{650} of the cultures, it was evident that at 36°C, the *GCD2 gcn3-101* strain incorporated radioactive leucine at a significantly higher rate per unit cell mass than the *gcd2-503 gcn3-101* mutant (Fig. 1B). These findings suggest that the *gcd2-503* mutation leads to a rapid reduction in the rate of protein synthesis following a shift to the nonpermissive temperature.

***gcd2-503 gcn3-101* mutants exhibit polysome profiles indicative of a reduced rate of translation initiation.** In an effort to determine whether translation initiation or elongation was impaired by the *gcd2-503* mutation at the nonpermissive temperature, we analyzed polysome profiles in *gcd2-503 gcn3-101* cells before and after a shift from 23 to 37°C. Figure 2A shows the results of sucrose gradient velocity sedimentation of cell extracts isolated from a control strain containing the *prt1-1* mutation. Analysis of the effects of this mutation in a cell-free translation system have revealed a specific defect in the ability to bind ternary complexes consisting of eIF-2, GTP, and Met-tRNA$_i^{Met}$ to small ribosomal subunits (13), an early step in the initiation of protein synthesis. When grown at 23°C, the *prt1-1* strain TP11B-4-1 showed a wild-type sedimentation profile of 80S monosomes and polysomes; however, after 15 min at 37°C, it exhibited a nearly complete loss of polysomes and a large accumulation of 80S particles (Fig. 2A). This effect has been attributed to a greatly reduced rate of initiation coupled with efficient completion of nascent polypeptide chains at the nonpermissive temperature (21). As expected, this runoff of polysomes was shown to be prevented by the addition of cycloheximide prior to the temperature shift at concentrations high enough to block elongation (21).

The *gcd2-503* mutation qualitatively resembled the *prt1-1* mutation in reducing the polysome/monosome ratio by more than a factor of 2 (from a ratio of 3.0 to 1.3) when the *gcd2-503 gcn3-101* mutant H625 was incubated at 37°C for 30 min (Fig. 2B). In addition, the average size of the polysomes remaining at the nonpermissive temperature was less than that of the polysomes present in the same strain grown at 23°C (see legend to Fig. 2B). The isogenic *GCD2 gcn3-101* strain H1459 showed no detectable change in either the polysome/monosome ratio or the average size of polysomes when incubated at 37°C for 30 min (Fig. 2C). As shown previously for a *prt1-1* mutant (21), addition of cycloheximide prior to the temperature shift eliminated the reduction in polysome content at 37°C in *gcd2-503 gcn3-101* strain H625 (Fig. 2B), implying that translation elongation is required for polysome runoff at 37°C in this mutant. Results indistinguishable from those shown in Fig. 2C for *GCD2 gcn3-101* strain H1459 were obtained for the isogenic *gcd2-503 GCN3* strain H1462 (data not shown), indicating that wild-type *GCN3* can overcome the defect in translation initiation evident in strain H625.

Many of the 80S particles that accumulate in the *gcd2-503 gcn3-101* strain at the nonpermissive temperature appear to be inactive 80S couples, in which 40S and 60S subunits interact in the absence of mRNA, rather than being 80S ribosomes engaged in translation. This conclusion follows from the experiment shown in Fig. 3, in which polysomes were fractionated on high-salt sucrose gradients containing 0.7 M NaCl. Under these conditions, 80S couples not associated with mRNA dissociate into 40S and 60S subunits, whereas 80S ribosomes engaged in translation are stable (34, 35). Incubation of *gcd2-503 gcn3-101* strain H625 at the nonpermissive temperature led to a significant accumulation of free 40S and 60S particles not seen in *GCD2 gcn3-101* strain H1459 under the same circumstances. Presumably, 80S couples accumulate in H625 at the restrictive temperature because the initiation factors responsible for preventing subunit association in the absence of mRNA (eIF-3 and eIF-6; 36, 45) are present in smaller amounts than the free ribosomal subunits (6).

In the high-salt gradients shown in Fig. 3, polysomes of different size are not well resolved (35); nevertheless, as in Fig. 2B, it is evident that the average size of polysomes remaining in *gcd2-503 gcn3-101* strain H625 at 37°C was

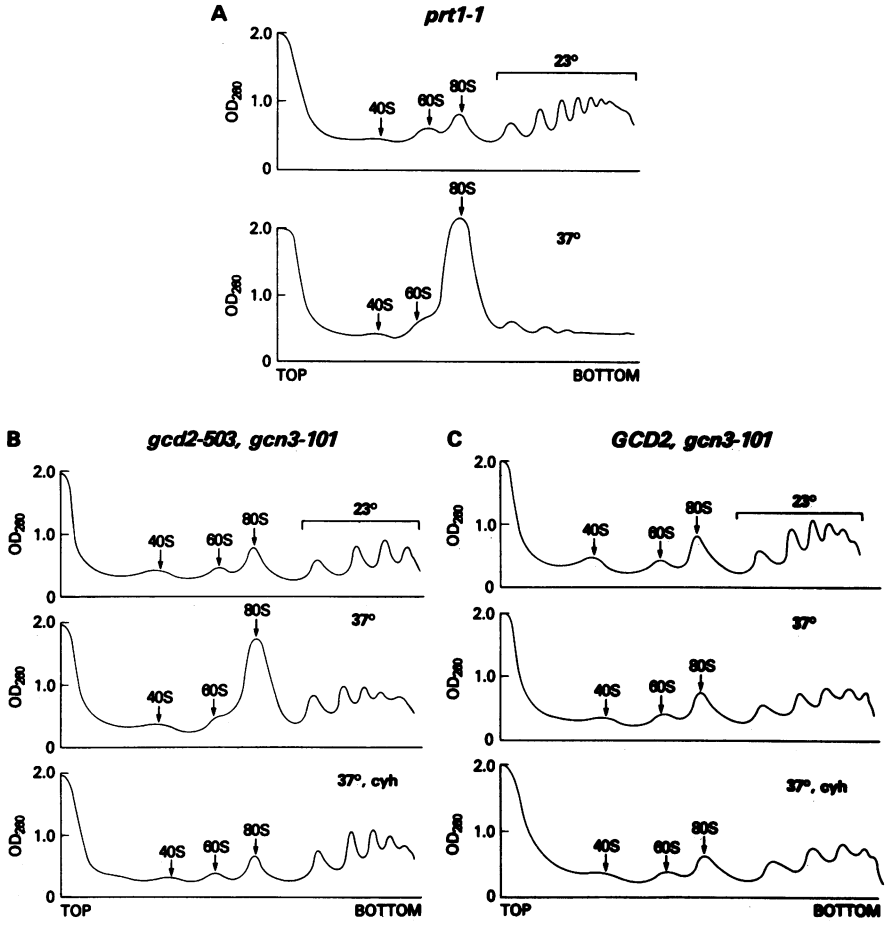

FIG. 2. Analysis of polysome profiles in *prt1-1*, *gcd2-503 gcn3-101*, and *GCD2 gcn3-101* yeast strains, using low-salt sucrose density gradient centrifugation. Extracts prepared from yeast strains grown in YPD medium at the indicated temperatures were centrifuged on low-salt 7 to 47% sucrose gradients for 2.5 h at 39,000 rpm. Gradients were fractionated while scanning at 254 nm, and the resulting absorbance profiles are shown, beginning with the top of the gradient on the left. The positions of 40S, 60S, and 80S ribosomal species are indicated. (A) Polysome profiles of the temperature-sensitive *prt1-1* mutant TP11B-4-1 grown at 23°C (top gradient) or 15 min after shifting from 23 to 37°C (bottom gradient). (B) Polysome profiles of the temperature-sensitive *gcd2-503 gcn3-101* strain H625 grown at 23°C (top gradient) or after shifting from 23 to 37°C for 30 min (middle gradient). For the bottom gradient, cycloheximide (cyh) was added to the culture just before shifting to 37°C. (C) Profile of isogenic *GCD2 gcn3-101* strain H1459, analyzed under the same conditions as strain H625 in panel B. In the "23°" gradient of panel B, 49% of the polysomal OD_{260} was in 2-mers and 3-mers; this proportion increased to 57% for the "37°" gradient. The corresponding values for the "23°" and "37°" gradients for the *GCD2* strain in panel C were 47 and 49%, respectively.

significantly less than in the isogenic *GCD2* strain H1459 at the same temperature. RNA blot hybridization analysis of *PYK1* mRNA showed no change in the steady-state level of the full-length transcript following the shift to 37°C in either strain (data not shown). Therefore, we attribute the reduction in the amount and average size of polysomes seen in the *gcd2-503 gcn3-101* mutant to a reduced rate of translation initiation, rather than a general reduction in mRNA synthesis or stability.

Evidence for accumulation of eIF-2 in preinitiation complexes in *gcd2-503 gcn3-101* mutants. Another observation consistent with the idea that translation initiation is defective at 37°C in a *gcd2-503 gcn3-101* mutant is shown in Fig. 4. Antibodies specific for the alpha subunit of eIF-2 (the product of *SUI2*) were used to localize eIF-2 in low-salt sucrose gradient fractionations of extracts made from the same strains analyzed in Fig. 2B and C. In the *GCD2 gcn3-101* strain H1459 incubated at either temperature, and in the *gcd2-503 gcn3-101* mutant H625 at 23°C, eIF-2α was found to be about equally distributed between one pool migrating on the heavy side of the 40S peak and another pool spread over several fractions closer to the top of the gradient. The more rapidly sedimenting pool probably represents 43S or 48S preinitiation intermediates containing eIF-2 · GTP · Met-$tRNA_i^{Met}$ ternary complexes and other initiation factors bound to 40S subunits; 48S complexes also contain mRNA (36, 46). Following the shift to 37°C in the *gcd2-503 gcn3-101* mutant, we consistently observed an increase in the proportion of the total eIF-2α that comigrated with the 40S subunits, increasing from 22 to 45% of the total amount present in the gradient for the experiment shown in Fig. 4. This finding suggests that a step in translation initiation following the formation of 43S or 48S preinitiation complexes is impaired in the *gcd2* mutant at the nonpermissive temperature, leading to accumulation of these complexes as reaction intermediates. Interestingly, the same phenomenon shown in Fig. 4 was observed for a temperature-sensitive *gcd1-101* mutant that resembles *gcd2-503*

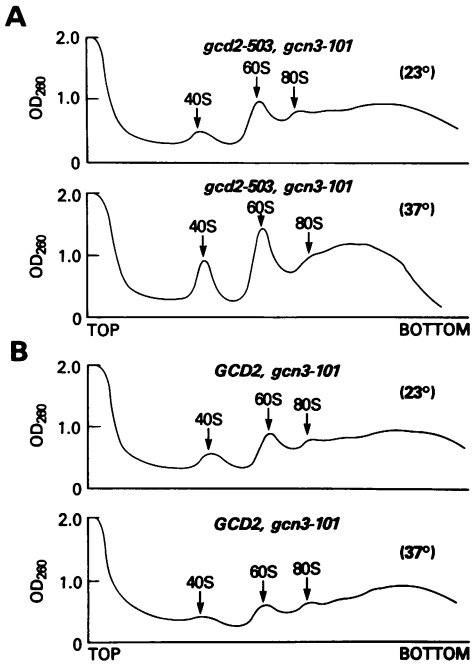

FIG. 3. Analysis of polysome profiles in *gcd2-503 gcn3-101* and *GCD2 gcn3-101* yeast strains by high-salt sucrose density gradient centrifugation. Extracts prepared from yeast strains grown exactly as described for Fig. 2 were centrifuged on high-salt 7 to 47% sucrose gradients for 2.5 h at 39,000 rpm and analyzed as for Fig. 2. (A) Polysome profiles of *gcd2-503 gcn3-101* mutant strain H625; (B) polysome profiles of the isogenic *GCD2 gcn3-101* strain H1459.

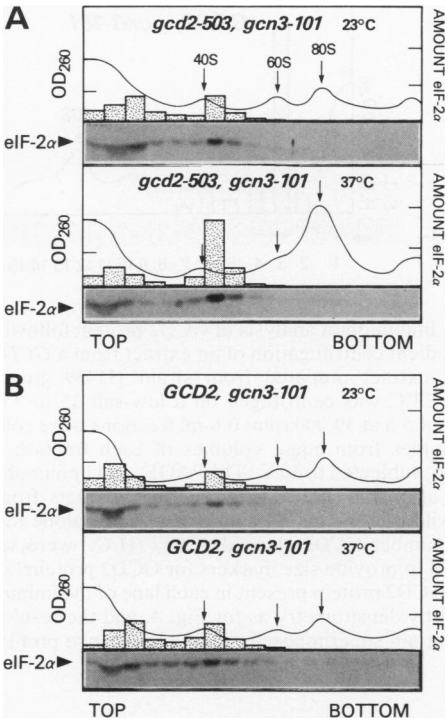

FIG. 4. Immunoblot analysis of eIF-2α following low-salt sucrose gradient centrifugation of extracts from *gcd2-503 gcn3-101* and *GCD2 gcn3-101* strains. Extracts prepared from the isogenic strains H625 and H1459 grown in YPD medium at 23°C or after shifting to 37°C for 30 min were centrifuged on low-salt 15 to 35% sucrose gradients for 4.5 h at 39,000 rpm. Gradients were fractionated from the top; 0.6-ml fractions were collected. Proteins were precipitated from equal volumes of each fraction, subjected to 10% SDS-PAGE, and analyzed by immunoblotting using antibodies against eIF-2α. The immunoblot was photographed, and the relative amounts of eIF-2α in the different fractions were quantitated by densitometry of the negative. The results are shown in the histogram superimposed on the absorbance profile in each panel.

gcn3-101 strain H625 in showing a reduced polysome content when incubated at the nonpermissive temperature (6a).

When fractions from a low-salt sucrose gradient fractionation of an extract made from *GCD2 gcn3-101* strain H1459 were analyzed by immunoblotting using GCD2-specific antiserum, we consistently found about 10% of the total GCD2 protein migrating in a peak located on the heavy side of the 40S ribosomal subunits (Fig. 5), similar in migration to the rapidly sedimenting species of eIF-2 shown in Fig. 4. The remainder of the GCD2 sedimented at approximately 15S. (The upper band present in the immunoblot of Fig. 5 was judged to be a nonspecific cross-reacting species based on the fact that its abundance was unaffected by increasing *GCD2* gene dosage or by *gcd2* mutations that destabilize GCD2 protein; data not shown.) Interestingly, the same bimodal distribution shown in Fig. 5 was observed for GCD1 and GCN3, and the 15S species has been shown to be a high-molecular-weight complex containing GCD1, GCD2, and GCN3 (6a). The localization of a fraction of GCD2 to the 40S region of the gradient, as shown in Fig. 5, supports the notion that GCD2 contributes to the formation or utilization of 43S or 48S preinitiation complexes. It was not possible to compare the localization of mutant and wild-type GCD2 proteins because the *gcd2-502* and *gcd2-503* gene products are unstable in cell extracts (data not shown).

Accumulation of halfmer polysomes in *gcd2-502 gcn3-101* mutants. Strain H1456 containing the *gcd2-502 gcn3-101* double mutation is thermosensitive for growth; however, this phenotype is less severe than that seen for the *gcd2-503 gcn3-101* mutant H625 analyzed above (data not shown). Comparison of extracts from isogenic *gcd2-502 gcn3-101* and *GCD2 gcn3-101* strains H1456 and H1457, respectively, on low-salt sucrose gradients revealed two differences with respect to polysomes (Fig. 6A). First, in the *gcd2-502 gcn3-101* mutant, the polysome/monosome ratio was only 1.4, compared with a value of 2.6 measured in the *GCD2 gcn3-101* strain. Second, discrete peaks were found migrating between the conventional polysomes. The unusual species present in the *gcd2-502 gcn3-101* mutant resemble halfmer polysomes produced by treatment with certain inhibitors of translation initiation that impair 40S-60S subunit joining in the last step of the initiation process (edeine, pactamycin, anisomycin, NaF, and cycloheximide at low concentration; 22, 26, 28, 29, 31, 53). Another situation that leads to halfmer polysomes is a deletion of one of the two genes *RPL16A* and *RPL16B* encoding the 60S subunit ribosomal protein L16 (47). This is illustrated in Fig. 6B for mutant strain H1532 containing the deletion/disruption allele of *RPL16B* known as *rpl16b*::*LEU2*. As shown below, this *rpl16b*::*LEU2* mutant has a higher 40S/60S subunit ratio than is seen for an isogenic wild-type *RPL16B* strain, presumably because of reduced amounts of 60S subunits in the mutant. Thus, the formation of halfmers in the *rpl16b*::*LEU2* mutant, and in response to the aforementioned inhibitors of initiation, can both be explained as the result of reduced 40S-60S subunit joining, leading to the accumulation of mRNA-bound 43S preinitiation complexes (47).

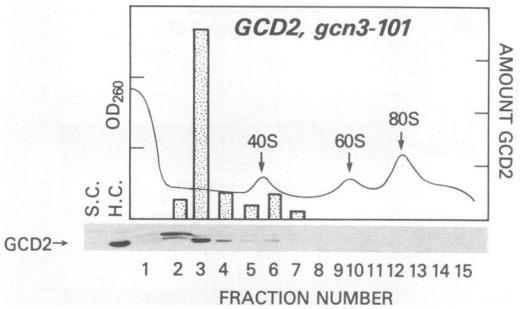

FIG. 5. Immunoblot analysis of GCD2 protein following low-salt sucrose gradient centrifugation of an extract from a *GCD2 gcn3-101* strain. An extract prepared from strain H1459 grown in YPD medium at 23°C was centrifuged on a low-salt 15 to 35% sucrose gradient for 4.5 h at 39,000 rpm; 0.6-ml fractions were collected, and protein samples from equal volumes of each fraction were TCA precipitated, subjected to 10% SDS-PAGE, and immunoblotted with antibodies against GCD2; 50 μg of crude extracts from transformants of wild-type strain H4 containing vector alone (S.C.) or the high-copy-number *GCD2* plasmid pCP57 (H.C.) were separated in the same gel to provide size markers for GCD2 protein (arrow). The amount of GCD2 protein present in each lane of the immunoblot was quantitated by densitometry as for Fig. 4, and the results are given in the histogram superimposed on the absorbance profile.

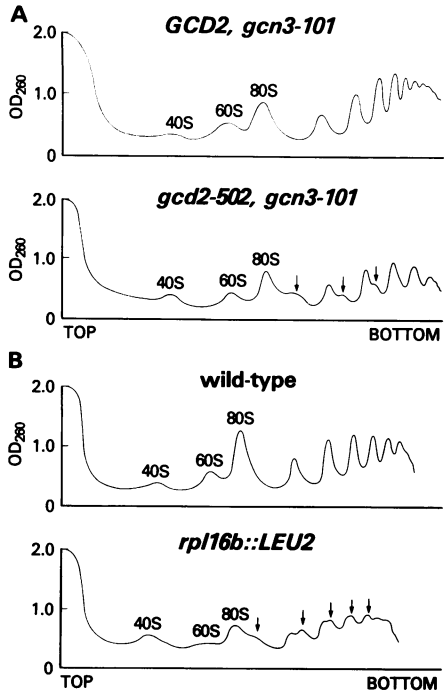

FIG. 6. Analysis of polysomes in *gcd2-502 gcn3-101*, *GCD2 gcn3-101*, and *rpl16b::LEU2* strains by low-salt sucrose gradient centrifugation. Extracts prepared from yeast strains H1457 (*GCD2 gcn3-101*) and H1456 (*gcd2-502 gcn3-101*) (A) and H1402 (*RPL16B*) and H1532 (*rpl16b::LEU2*) (B), grown in YPD medium at 23°C, were centrifuged on low-salt 7 to 47% sucrose gradients for 2.5 h at 39,000 rpm and analyzed as for Fig. 2. The arrows in the bottom part of each panel indicate the halfmer polysomal species.

In an effort to demonstrate that the halfmer polysomes which accumulate in *gcd2-502 gcn3-101* strain H1456 contain an extra 40S subunit, we determined the relative amounts of 18S and 25S rRNA in fractions of the sucrose gradient containing the putative halfmer species found on the heavy shoulder of the 80S peak. Total RNA was isolated from these fractions and analyzed by blot hybridization analysis using the yeast ribosomal DNA repeat as a hybridization probe (data not shown). The ratio of 18S rRNA/25S rRNA measured for the *GCD2 gcn3-101* strain H1457 ranged between 0.8 and 1.4 for several different fractions on the heavy side of the 80S peak; by contrast, this ratio was significantly greater in the corresponding position of the gradient from the *gcd2-502 gcn3-101* mutant, with ratios ranging between 2.3 and 4.0 for the halfmer-containing fractions. These results support the idea that the halfmer polysomes observed in the *gcd2-502 gcn3-101* mutant contain 40S ribosomal subunits unassociated with 60S subunits, in addition to 80S ribosomes. The observation that the halfmer-containing fractions exhibit 18S rRNA/25S rRNA ratios more than twofold greater than the normal ratio for 80S ribosomes might indicate that more than one free 40S subunit is bound to the halfmer polysomes.

Both the reduced polysome/monosome ratio and the presence of halfmer polysomes were observed in the *gcd2-502 gcn3-101* strain H1456 about equally at 23°C and after 30 min of incubation at 37°C. However, after prolonged incubation of this mutant at 37°C (40 to 60 min), the total polysome content decreased even further, the halfmer species became less pronounced, and 80S particles accumulated (data not shown). These results suggest that polysome runoff is a more severe manifestation of the *gcd2-502* mutation than the formation of halfmers. The isogenic *gcd2-502 GCN3* strain H1458 did not accumulate halfmer polysomes at either temperature (data not shown).

Formation of halfmers in the *gcd2-502 gcn3-101* mutant does not result from ribosomal subunit imbalance. The presence of halfmer polysomes containing extra 40S subunits in the *gcd2-502 gcn3-101* mutant could result from a defect in a late step of the initiation pathway, following binding of 43S preinitiation complexes to mRNA. Alternatively, it was formally possible that the *gcd2-502* mutation leads to a greater 40S/60S subunit ratio than in wild-type cells, as occurs in *rpl16b::LEU2* strains. The latter possibility was eliminated by measuring the relative amounts of 40S and 60S subunits on sucrose gradients containing low concentrations of Mg^{2+}, in which polysomes and 80S ribosomes dissociate into free ribosomal subunits. As shown in Fig. 7A and 7B, the isogenic *gcd2-502 gcn3-101* and *GCD2 gcn3-101* strains H1456 and H1457, respectively, had very similar amounts of 40S and 60S subunits, and the 40S/60S mass ratio was 0.60 for both strains. By contrast, the *rpl16b::LEU2* mutation in strain H1532 led to an increase in the 40S/60S ratio from 0.6 to 0.8 (Fig. 7C and D). Note that an isogenic strain (H1654) containing a deletion of the small subunit ribosomal protein gene *RP51A* showed a decreased 40S/60S ratio of 0.3 (Fig. 7E), presumably because of low levels of RP51 protein and 40S ribosomal subunits (2). On the basis of these findings, we conclude that the presence of halfmer polysomes in the *gcd2-502 gcn3-101* mutant is not due to low levels of 60S subunits. Rather, it appears to result from a defect late in the initiation pathway following the binding of 43S preinitiation complexes to mRNA. We also showed that the 40S/60S mass ratio in the *gcd2-503 gcn3-101* strain H625 was the same either at 23°C or following a shift to 36°C, indicating that the reduced initiation rate seen in this mutant at the nonpermissive temperature does not result from ribosomal subunit imbalance (data not shown).

Deletion of the 60S subunit ribosomal protein gene *RPL16B*

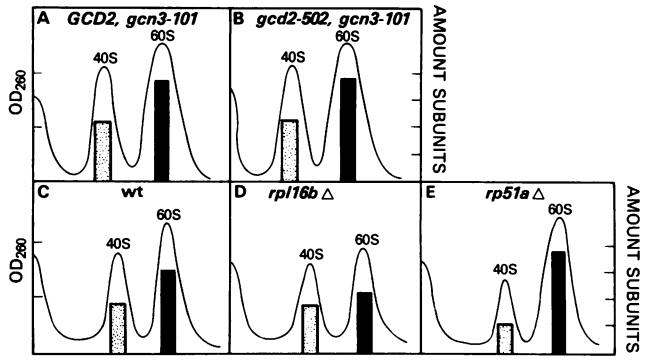

FIG. 7. Analysis of the amounts of 40S and 60S subunits in wild-type and mutant yeast strains by centrifugation on low-Mg^{2+} sucrose density gradients. Extracts prepared from the strains indicated below grown in YPD medium at 23°C were centrifuged on low-Mg^{2+} 7 to 47% sucrose gradients for 2.5 h at 39,000 rpm. Gradients were fractionated from the top while scanning at 254 nm, and the total absorbance in the 40S and 60S peaks is shown by the histograms superimposed on the absorbance profiles. (A) Strain H1457 (*GCD2 gcn3-101*); (B) strain H1456 (*gcd2-502 gcn3-101*); (C) strain H1402 (*RPL16B*); (D) strain H1532 (*rpl16b*::*LEU2*); (E) strain H1654 (*rp51a*::*LEU2*).

impairs translational control of *GCN4*. Even though the halfmer polysomes observed in the *gcd2-502 gcn3-101* mutant do not result from reduced amounts of 60S subunits, it was of interest to know whether the reduced rate of 40S-60S joining that occurs in a *rpl16b*::*LEU2* mutant leads to derepression of *GCN4* translation, similar to that seen in *gcd* mutants. This question was of particular interest in view of the model we recently proposed for *GCN4* translational control (1) (Fig. 8). According to this model, ribosomes translate uORF1 and the 40S subunits remain attached to the mRNA leader and resume scanning downstream. Under nonstarvation conditions, all of these 40S subunits reinitiate at uORFs 2 to 4 and fail to reinitiate at *GCN4*. Under starvation conditions, or in *gcd* mutants, many of the 40S subunits ignore the start codons at uORFs 2 to 4 and reinitiate at *GCN4* instead. This is thought to occur because the reassembly of initiation complexes following termination at uORF1 is slower under starvation conditions and thus requires a greater scanning time. Consequently, a fraction of 40S subunits scanning downstream from uORF1 becomes competent to reinitiate only after bypassing uORFs 2 to 4, while scanning the leader sequences between uORF4 and *GCN4*. A corollary of this model is that the low levels of 60S subunits associated with the *rpl16b*::*LEU2* deletion should increase the number of 43S preinitiation complexes that scan past uORFs 2 to 4 and reinitiate at *GCN4* under nonstarvation conditions (Gcd^- phenotype). Such an effect should be independent of GCN1, GCN2, and GCN3, the positive regulators of *GCN4* translation, as these factors are thought to retard the reassembly of an initiation complex, not the availability of 60S subunits.

The first observation we made supporting the above corollary was that the *rpl16b*::*LEU2* deletion mimicked *gcd* mutations in restoring derepression of *HIS3* gene expression in *gcn2* and *gcn3* mutants. Mutations in *GCN2* and *GCN3* prevent derepression of genes encoding enzymes in the histidine pathway that are under the positive control of *GCN4*, such as *HIS3*. Consequently, *gcn2* and *gcn3* mutants are sensitive to 3-AT, an inhibitor of the *HIS3* gene product (25). Replacement of *RPL16B* with the *rpl16b*::*LEU2* deletion allele in *gcn2*::*URA3* strain H1333 and in *gcn3*::*URA3* strain H1550 suppressed the 3-AT sensitivity associated with the *gcn* mutations in these strains (Fig. 9). In addition, when the *gcn3*::*URA3 rpl16b*::*LEU2 leu2* strain H1555 was

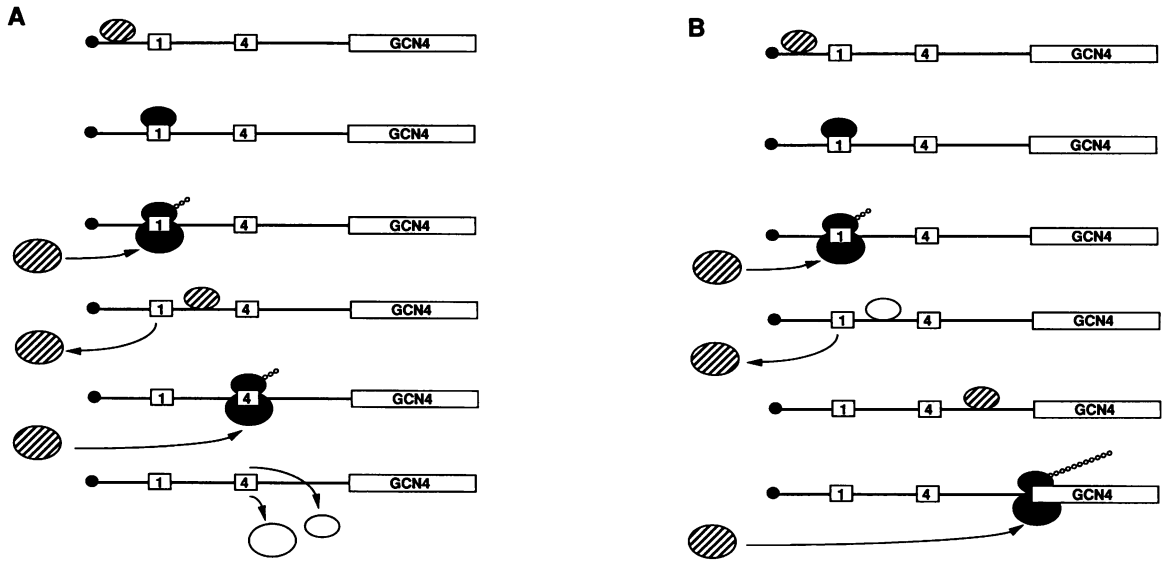

FIG. 8. Model for *GCN4* translational control. The *GCN4* transcript is shown with uORFs 1 and 4 and the *GCN4* coding region depicted as labeled boxes (uORFs 2 and 3 are dispensable for regulation [38]). Large and small ribosomal subunits are shown hatched when they are competent to initiate and solid when elongating; unshaded 40S subunits lack one or more factors needed to reinitiate translation. (A) Under nonstarvation conditions, ribosomes translate uORF1 and 40S subunits resume scanning. The necessary initiation factors are reassembled rapidly, and reinitiation occurs efficiently at uORF4. Following termination at this site, both subunits dissociate from the mRNA, preventing translation of *GCN4*. (B) Under starvation conditions, reassembly of a competent initiation complex following translation of uORF1 occurs more slowly, allowing 50% of the 40S subunits to ignore the uORF4 AUG codon; these subunits become competent to reinitiate after scanning the additional sequences in the uORF4-*GCN4* interval and initiate translation at *GCN4* instead.

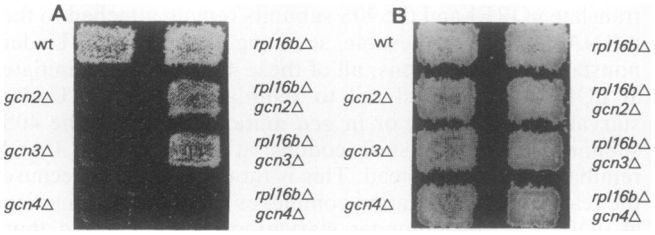

FIG. 9. Growth of *gcn* and *rpl16b*::*LEU2* strains under histidine starvation and nonstarvation conditions. Strains with the indicated relevant genotype were grown on SD medium for 3 days at 30°C, replica printed to SD containing 3-AT for histidine starvation (A) and to SD for nonstarvation conditions (B), and incubated for 2 days at 30°C. The following strains were analyzed: wild-type (wt), H1402; *gcn2*Δ, H1333; *gcn3*Δ, H1550; *gcn4*Δ, H1652; *rpl16b*Δ, H1532; *rpl16b*Δ *gcn2*Δ, H1533; *rpl16b*Δ *gcn3*Δ, H1555; and *rpl16b*Δ *gcn4*Δ, H1653.

crossed by *gcn3*::*URA3 RPL16B leu2* strain H1550 and the resulting diploid was sporulated and subjected to tetrad analysis, we obtained two 3-AT-resistant Leu$^+$ and two 3-AT-sensitive Leu$^-$ ascospores from each of ten asci dissected. These results suggest that the *rpl16b*::*LEU2* mutation restores derepression of *HIS3* expression under starvation conditions in *gcn2* and *gcn3* mutants. By contrast, the *rpl16b*::*LEU2* deletion did not suppress the 3-AT sensitivity associated with a *gcn4*::*URA3* mutation (Fig. 9), as expected if the increased *HIS3* expression resulting from the *rpl16b*::*LEU2* deletion is mediated by GCN4 protein.

The *rpl16b*::*LEU2* deletion also led to increased resistance to 5-fluorotryptophan (5-FT), a compound that competes with tryptophan for incorporation into proteins but does not trigger the derepression of enzymes subject to the general control (Table 3). *gcd* mutations result in constitutive enzyme derepression and resistance to 5-FT due to elevated tryptophan levels under nonstarvation conditions (39, 54). The 5-FT resistance associated with the *rpl16b*::*LEU2* deletion suggests that this mutation leads to increased expression

TABLE 3. Derepression associated with the *rpl16b*::*LEU2* mutation of tryptophan and histidine biosynthetic enzymes independent of *GCN2* and *GCN3* but dependent on *GCN4* function

Strain	Relevant genotype	Growth[a] on:		HIS4-LacZ activity[b] (U)	
		5-FT	3-AT	R	DR
H1402[c]	Wild type	−/+	+	90	500
H1532[c]	*rpl16b*::*LEU2*	+	+	230	260
H1333[c]	*gcn2*::*URA3*	−	−	62	45
H1533[c]	*rpl16b*::*LEU2 gcn2*::*URA3*	+	+	210	330
H1550	*gcn3*::*URA3*	−	−	100	66
H1555	*rpl16b*::*LEU2 gcn3*::*URA3*	+	+	360	240
H1652[c]	*gcn4*::*URA3*	−	−	40	14
H1653[c]	*rpl16b*::*LEU2 gcn4*::*URA3*	−	−	40	19
H1654[c]	*rp51a*::*LEU2*	−/+	+	88	370
H1489[c]	*gcn3*[c]*R104K*	+	+	960	1,000

[a] Strains were replica printed to 5-FT (0.5 mM) or 3-AT (30 mM) medium and scored for growth at 30°C after 1 to 2 days. +, confluent growth; −/+, very weak growth; −, no visible growth.

[b] β-Galactosidase activity was assayed under repressing (R, nonstarvation) and derepressing (DR, histidine starvation) conditions. Values are averages of results obtained from assays on two to three independently derived transformants; for each construct, the individual measurements deviate from the average value by 30% or less.

[c] Isogenic strains.

TABLE 4. Evidence that efficient derepression of *GCN4-lacZ* in a *rpl16b*::*LEU2* mutant requires multiple upstream AUG codons in the *GCN4* mRNA leader[a]

Strain	Relevant genotype	GCN4-LacZ activity (U)					
		p180 (uORFs 1–4)		p226 (uORF4 only)		p227 (no uORFs)	
		R	DR	R	DR	R	DR
H1511	*RPL16B*	16	130	9	24	720	840
H1657	*rpl16b*::*LEU2*	52	72	19	20	1,200	1,200

[a] The analysis was conducted as for Table 3.

of tryptophan biosynthetic enzymes under nonstarvation conditions. This phenotype is not affected by inactivation of *GCN2* or *GCN3* but is completely dependent on *GCN4* (Table 3). In summary, the pattern of resistance to 3-AT and 5-FT associated with the *rpl16b*::*LEU2* deletion indicates that this mutation resembles *gcd* mutations in causing increased expression of *GCN4* and genes under its control in the absence of both amino acid starvation and the positive regulators *GCN2* and *GCN3*.

This conclusion was supported by measuring the expression of a *HIS4-lacZ* fusion present in the strains analyzed in Table 3. Under nonstarvation conditions (column R), the *rpl16b*::*LEU2* deletion led to 2.5-fold-higher *HIS4-lacZ* expression in strain H1532 than in the isogenic *RPL16B* strain H1402 and more than 3-fold-higher *HIS4-lacZ* expression in the *gcn2*::*URA3* and *gcn3*::*URA3* strains H1533 and H1555 than in their respective *RPL16B* parents H1333 and H1550. As expected, *rpl16b*::*LEU2* led to no derepression in the *gcn4*::*URA3* strain H1653 relative to its *RPL16B* parent H1652. Surprisingly, under histidine starvation conditions, the *rpl16b*::*LEU2* deletion led to lower *HIS4-lacZ* expression in strain H1532 compared with that in the parental *RPL16B* strain H1402 (Table 3). As a result, *HIS4-lacZ* was constitutively derepressed at an intermediate level in H1532. By contrast with the latter findings, *gcd* mutations (25) and constitutively derepressing alleles of *GCN3* (16) generally derepress *HIS4-lacZ* expression to levels exceeding that seen in wild-type cells grown in the presence of 3-AT (e.g., strain H1489 in Table 3). Deletion of the small subunit ribosomal protein gene *RP51A* from wild-type strain H1402 had little or no effect on the regulation of *HIS4-lacZ*: under derepressing conditions, expression was reduced by 25%; however, the derepression ratio remained high (DR/R = 4.1) (Table 3). Thus, the partial derepression of *HIS4-lacZ* expression seen in the *rpl16b*::*LEU2* deletion mutant H1532 appears to result specifically from insufficient amounts of 60S ribosomal subunits.

Measurements of *GCN4-lacZ* expression in the isogenic *RPL16B* and *rpl16b*::*LEU2* strains H1511 and H1657 exhibited the same trends shown in Table 3 for *HIS4-lacZ* expression, indicating that *rpl16b*::*LEU2* impairs the regulation of amino acid biosynthetic genes by altering *GCN4* expression: GCN4-LacZ enzyme activity from plasmid p180 containing the wild-type *GCN4* mRNA leader was partially derepressed under nonstarvation conditions in the *rpl16b*::*LEU2* mutant compared with the *RPL16B* strain (Table 4). Under starvation conditions, *GCN4-lacZ* expression was lower in the *rpl16b*::*LEU2* strain than in the wild type. Removal of the first three or all four uORFs from the *GCN4* mRNA leader diminished the effects of the *rpl16b*::*LEU2* deletion on *GCN4-lacZ* expression (Table 4). These latter

results suggest that *rpl16b*::*LEU2* alters *GCN4* expression largely by disrupting the normal mechanism of translational control, as its effects are dependent on the number of uORFs present in the leader (25). The opposing influences of the *rpl16b*::*LEU2* mutation on *GCN4* expression under starvation versus nonstarvation conditions will be discussed below in the context of our model for *GCN4* translational control.

DISCUSSION

Function of GCD2 in general translation initiation. GCD2 was first identified as a negative regulator of *GCN4* expression that is required for the inhibitory effects of the uORFs on translation initiation at *GCN4* under nonstarvation conditions. Because *gcd2* mutations overcome the requirement for GCN1, GCN2, and GCN3 for increased translation of *GCN4* mRNA, it was proposed that the repressing function of GCD2 is antagonized by these positive-acting factors in amino acid-starved cells (25). Presumably, this antagonism is not complete, as *GCD2* is an essential gene (41). Allele-specific interactions between mutations in *GCD1* and *GCD2* with *GCN3* led to the proposal that these positive and negative regulators closely interact in controlling *GCN4* expression (19, 40). Recent biochemical studies support this proposal in showing that GCD1, GCD2, and GCN3 are present in a high-molecular-weight complex that appears to interact with a specific fraction of the eIF-2 in the cell (6a). The latter finding was presaged by the observation that certain mutations in *SUI2* and *SUI3*, the structural genes for eIF-2α and eIF-2β, respectively, resemble *gcd* mutations in causing constitutive derepression of *GCN4*. In addition, the *sui2-1* mutation is unconditionally lethal in combination with a *gcn3* deletion (54), just as temperature-sensitive lethal mutations in *GCD1* and *GCD2* are exacerbated by deletion of *GCN3* (19, 17). Thus, considerable genetic and biochemical evidence exists that GCD1, GCD2, and GCN3 have general functions in protein synthesis involving eIF-2, in addition to their gene-specific roles in regulating translation of *GCN4* mRNA.

The results presented in this report support this conclusion in showing that strains containing temperature-sensitive lethal *gcd2* mutations exhibit several phenotypes indicative of defects in general protein synthesis: (i) sensitivity to inhibitors of protein synthesis (Table 2); (ii) reduced incorporation of radioactive leucine into total cell protein (Fig. 1); (iii) polysome runoff and accumulation of eIF-2α in 43S-48S particles (in *gcd2-503 gcn3-101* cells) (Fig. 2 to 4); and (iv) halfmer polysomes containing extra 40S ribosomal subunits bound to mRNA (in *gcd2-502 gcn3-101* cells) (Fig. 6). As discussed below, the latter two phenotypes are consistent with a specific defect at a late step in the translation initiation pathway. These defects were eliminated by replacing *gcn3-101* with wild-type *GCN3*, in accord with the idea that under nonstarvation conditions, the positive regulator GCN3 contributes to the essential function of GCD2 in translation initiation.

The presence of halfmer polysomes containing extra ribosomal subunits bound to mRNA in the *gcd2-502 gcn3-101* mutant (Fig. 6A) suggests that one of the steps between mRNA binding by the 43S preinitiation complex and subunit joining with the 60S subunit at the AUG codon occurs less efficiently in this mutant. The impaired step could be scanning or recognition of the AUG codon, hydrolysis of GTP in the ternary complex, release of eIF-2 · GDP, or 40S-60S subunit joining (36). Because one of these steps occurs at a reduced rate, preinitiation complexes persist long enough to be detected on polysomes, forming halfmer species. It is noteworthy that cycloheximide at low concentrations is one of several drugs that inhibit 40S-60S subunit joining and thereby produce halfmer polysomes (22) and, as shown in Table 2, *gcd2-1* and *gcd2-503 gcn3-101* mutants are sensitive to cycloheximide.

The accumulation of eIF-2 in the 43S-48S region seen for the *gcd2-503 gcn3-101* mutant at the nonpermissive temperature (Fig. 4) is consistent with the idea that GCD2 contributes to a step in the initiation pathway following the binding of eIF-2 · GTP · Met-tRNA$_i^{Met}$ ternary complexes to small ribosomal subunits. The *gcd1-101* mutation also leads to polysome runoff and accumulation of eIF-2 in the 43S-48S region (6a) similar to that shown in Fig. 4 for the *gcd2-503 gcn3-101* strain. If we assume that the eIF-2-containing species that accumulate in *gcd2-503 gcn3-101* and *gcd1-101* mutants at 37°C are 48S complexes containing mRNA, then *gcd1-101*, *gcd2-502*, and *gcd2-503* mutations could all lead to defects late in the initiation pathway. In this view, the *gcd2-503* and *gcd1-101* mutations lead to polysome runoff rather than halfmer formation at the nonpermissive temperature because the rate of initiation is more impaired by these mutations than by *gcd2-502*. With polysome runoff occurring in the *gcd2-503* and *gcd1-101* mutants, the accumulated preinitiation complexes would sediment primarily at 48S rather than forming halfmer polysomes. A similar effect has been observed in rabbit reticulocyte lysates containing an inhibitor of translation initiation from sea urchin eggs: these lysates are depleted of polysomes and show significant accumulation of 80S particles and 48S preinitiation intermediates (18). Consistent with this explanation is the fact that the *gcd2-502 gcn3-101* mutant exhibits halfmer polysomes at 23°C (Fig. 6A) when the growth rate is only slightly lower than that of wild-type cells; however, following prolonged incubation at 37°C, polysome runoff and 80S accumulation become more evident, presumably reflecting a more severe reduction in the rate of translation initiation.

Another observation consistent with a late step in the initiation process being defective in *gcd1* and *gcd2* mutants is the fact that *SUI2* and *SUI3* mutations with a Gcd$^-$ phenotype (derepressed expression of *GCN4*) were selected on the basis of their ability to utilize non-AUG start codons at *HIS4* (7, 11, 54). Thus, these mutations appear to affect a function of eIF-2 involved either in AUG codon recognition during the scanning process or in 80S initiation complex formation at the start codon, rather than the formation of ternary complexes or binding of these complexes to small ribosomal subunits. Similarly, the *rpl16b*::*LEU2* deletion mimics *gcd* mutations in causing derepression of *GCN4* expression under nonstarvation conditions (Table 3), and this mutation almost certainly leads to reduced rates of 40S-60S joining due to insufficient amounts of 60S subunits (Fig. 6 and 7). However, as discussed below, the effect of the *rpl16b*::*LEU2* deletion on *GCN4* expression appears to be more complex than that of known *gcd* and *SUI* mutations.

Effects of *gcd2* mutations on translation of *GCN4* mRNA. The possibility that *gcd* mutations reduce the efficiency of a late step in the initiation pathway has important implications for the mechanism of *GCN4* translational control. According to our model (1), under starvation conditions a substantial fraction of 40S subunits scanning downstream from uORF1 have not reassembled the factors needed for initiation by the time they reach uORFs 2 to 4 and become competent to reinitiate only after scanning the uORF4-*GCN4* interval (Fig. 8). This reassembly process requires more time under starvation conditions than under nonstarvation conditions be-

cause of reduced activity of one or more initiation factors that must associate with, or modify, the 40S subunit as it scans between uORF1 and *GCN4*. We previously suggested that the level of eIF-2 · GTP · Met-tRNA$_i^{Met}$ ternary complexes or the ability of these complexes to bind to 40S subunits would be reduced under starvation conditions, such that a substantial number of subunits will lack ternary complexes when they reach uORF4 (1). This possibility is consistent with the derepressed (Gcd$^-$) phenotype of certain mutations in *SUI2* and *SUI3* (54) and the depletion of ternary complexes bound to small ribosomal subunits observed in *gcd1-101* mutants at the restrictive temperature or after a nutritional shift-down in wild-type cells (52).

However, the accumulation of mRNA-bound preinitiation complexes (halfmer polysomes) and free 40S subunits containing eIF-2 in *gcd2* and *gcd1* mutants seen in our experiments suggests that derepression of *GCN4* involves a reduction in a late step of the initiation pathway, such as recognition of the AUG codon, eIF-2 · GTP hydrolysis to eIF-2 · GDP, release of eIF-2 · GDP at the AUG start codon, or 40S-60S subunit joining. In this view, 40S subunits containing eIF-2 · GTP · Met-tRNA$_i^{Met}$ ternary complexes scanning downstream from uORF1 have a reduced capacity to complete the formation of an 80S initiation complex, increasing the probability of bypassing uORFs 2 to 4. This deficiency would necessarily diminish with time so that efficient reinitiation at *GCN4* would occur after the subunits have scanned the additional sequences in the uORF4-*GCN4* interval. For example, interaction of another initiation factor (e.g., eIF-5; 43) with 43S complexes scanning downstream from uORF1 might have to occur before joining with a 60S subunit could take place at the next start site. eIF-2 would still play an important role in derepression of *GCN4* because the formation of 80S initiation complexes can occur only after eIF-2 · GDP is released from 43S preinitiation intermediates (48).

An initiation factor known as eIF-2B or GEF (guanine nucleotide exchange factor), which is required for recycling of eIF-2 · GDP to eIF-2 · GTP, has been shown to be the target of negative regulation in several cases in which protein synthesis is inhibited in mammalian cells (23, 48). In every case, it appears that eIF-2B is inhibited indirectly by phosphorylation of the α subunit of eIF-2. Phosphorylated eIF-2 · GDP forms a stable complex with eIF-2B that is inactive for recycling activity. It is intriguing that inhibition of eIF-2B activity in this manner appears to produce an accumulation of free 48S complexes and halfmer polysomes, suggesting that a late step in the initiation pathway is impaired (9, 10, 14, 15). This has led to the suggestion that eIF-2B is involved in removing eIF-2 · GDP from the ribosome in addition to converting eIF-2 · GDP to eIF-2 · GTP. The fact that *gcd1* and *gcd2* mutants accumulate initiation intermediates similar to those seen in eIF-2B-inhibited lysates is particularly interesting since the molecular weight of the complex containing GCD1, GCD2, and GCN3 and the association of this complex with eIF-2 raise the possibility that GCD1 and GCD2 are subunits of the yeast equivalent of eIF-2B (6a). If this hypothesis is correct, the GCN2 protein kinase may stimulate *GCN4* translation by phosphorylation of eIF-2 or one of the components of the GCD1/GCD2/GCN3 complex, thereby reducing the functions of eIF-2B involved late in the initiation pathway.

Deletion of *RPL16B* and *gcd* mutations differ in their effects on *GCN4* expression. The *rpl16b*::*LEU2* deletion resembles *gcd* (37) and *gcn3*^{c} (16) mutations in causing derepression of *GCN4* in the absence of starvation; however, the extent of derepression is smaller for *rpl16b*::*LEU2* than for these other mutations. In addition, under starvation conditions, *rpl16b*::*LEU2* prevents derepression of *GCN4* to the level seen in wild-type cells. Both phenotypes can be accounted for in the context of our model for *GCN4* translational control as a consequence of reducing the probability of 40S-60S subunit joining during the reinitiation process, not only at uORFs 2 to 4 but at *GCN4* as well. The depletion of 60S subunits caused by the *rpl16b*::*LEU2* mutation should allow a certain fraction of fully assembled 43S preinitiation complexes scanning downstream from uORF1 to scan past each of the uORFs without forming an 80S initiation complex. Because uORFs 2 to 4 must all be bypassed to reach *GCN4*, and because a fraction of the preinitiation complexes that reach *GCN4* will likewise fail to initiate there, only a modest increase in *GCN4* expression is expected to result from the *rpl16b*::*LEU2* deletion under nonstarvation conditions. In wild-type cells under starvation conditions, many 40S subunits scanning downstream from uORF1 have not assembled a preinitiation complex by the time they reach uORFs 2 to 4 and become competent to reinitiate only while traversing the uORF4-*GCN4* interval. Therefore, reducing the concentration of 60S subunits by the *rpl16b*::*LEU2* deletion should lead to a much smaller increase in the number of preinitiation complexes that reach *GCN4* under starvation conditions than under nonstarvation conditions. Moreover, since nearly all of the 40S subunits that ignore uORFs 2 to 4 appear to reinitiate at *GCN4* (1), the main effect of lowering the level of 60S subunits under starvation conditions may be to increase the number of 43S preinitiation complexes that bypass the *GCN4* start site, thereby reducing translation of *GCN4*. It is also possible that the *rpl16b*::*LEU2* deletion lowers *GCN4* expression under starvation conditions by decreasing the probability of initiation at uORF1, as ribosomes must translate this first uORF in order to reach *GCN4* (1, 25).

The *gcd* mutations are thought to reduce the rate at which 40S subunits re-form a preinitiation complex following termination at uORF1. Therefore, the efficiency of reinitiation is differentially affected at uORFs 2 to 4 versus *GCN4* due to the greater scanning time involved in reaching the latter start site (1). By contrast, the above explanation suggests that impairing the subunit joining reaction by reducing the concentration of 60S subunits in the *rpl16b*::*LEU2* strain lowers the efficiency of reinitiation equivalently at uORFs 2 to 4 and at *GCN4*, independent of the time required for 40S subunits to reach each site. Thus, the difference in the extent of derepression produced by *rpl16b*::*LEU2* and *gcd* mutations reinforces a central idea of our model, namely, that GCD factors contribute to a time-dependent modification of the 40S subunit during the scanning process that readies it for reinitiation downstream from uORF1 (1).

ACKNOWLEDGMENTS

We thank Thomas Dever, Ernie Hannig, Rosemary Jagus, Charles Moehle, Manuel Ramirez, Ron Wek, and John Woolford for their helpful comments on the manuscript, Kathy Shoobridge for help in its preparation, and our colleagues in the LMG for stimulating discussions. We are grateful to John Woolford, Nadja Abovich, Gerald Johnston, Ernie Hannig, and Paul Miller for gifts of yeast strains and plasmids.

REFERENCES

1. **Abastado, J. P., P. F. Miller, B. M. Jackson, and A. G. Hinnebusch.** 1991. Suppression of ribosomal reinitiation at upstream open reading frames in amino acid-starved cells forms the basis for *GCN4* translational control. Mol. Cell. Biol. **11**:486–496.

2. **Abovich, N., L. Gritz, L. Tung, and M. Rosbash.** 1985. Effect of *RP51* gene dosage alterations on ribosome synthesis in *Saccharomyces cerevisiae*. Mol. Cell. Biol. **5**:3429–3435.
3. **Baliga, B. S., A. W. Pronczuk, and H. N. Munro.** 1969. Mechanism of cycloheximide inhibition of protein synthesis in a cell free system prepared from rat liver. J. Biol. Chem. **244**:4480–4489.
4. **Boeke, J. D., F. LaCroute, and G. R. Fink.** 1984. A positive selection for mutants lacking orotidine-5'-phosphate decarboxylase activity in yeast: 5-fluoro-orotic acid resistance. Mol. Gen. Genet. **197**:345–346.
5. **Botstein, D., S. C. Falco, S. E. Stewart, M. Brennan, S. Scherer, D. T. Stinchcomb, K. Struhl, and R. W. Davis.** 1979. Sterile host yeasts (SHY): a eukaryotic system of biological containment for recombinant DNA experiments. Gene **8**:17–24.
6. **Browning, K. S., J. Humphreys, W. Hobbs, G. B. Smith, and J. M. Ravel.** 1990. Determination of the amounts of the protein synthesis initiation and elongation factors in wheat germ. J. Biol. Chem. **265**:17967–17973.

6a. **Cigan, A. M., M. Foiani, E. M. Hannig, and A. G. Hinnebusch.** 1991. Complex formation by positive and negative translational regulators of *GCN4*. Mol. Cell. Biol. **11**:3217–3228.

7. **Cigan, A. M., E. K. Pabich, L. Feng, and T. F. Donahue.** 1989. Yeast translation initiation suppressor *sui2* encodes the alpha subunit of eukaryotic initiation factor 2 and shares identity with the human alpha subunit. Proc. Natl. Acad. Sci. USA **86**:2784–2788.
8. **Cooper, T. G., and J. Bossinger.** 1976. Selective inhibition of protein synthesis initiation in *Saccharomyces cerevisiae* by low concentration of cycloheximide. J. Biol. Chem. **251**:7278–7280.
9. **De Benedetti, A., and C. Baglioni.** 1983. Phosphorylation of initiation factor eIF2alpha, binding of mRNA to 48S complexes, and its reutilization in initiation of protein synthesis. J. Biol. Chem. **258**:14556–14562.
10. **De Benedetti, A., and C. Baglioni.** 1984. Inhibition of mRNA binding to ribosomes by localized activation of dsRNA-dependent protein kinase. Nature (London) **311**:79–81.
11. **Donahue, T. F., A. M. Cigan, E. K. Pabich, and B. Castilho-Valavicius.** 1988. Mutations at a Zn(ll) finger motif in the yeast e1F-2β gene alter ribosomal start-site selection during the scanning process. Cell **54**:621–632.
12. **Feinberg, A. P., and B. Vogelstein.** 1984. Addendum: a technique for radiolabeling DNA restriction endonuclease fragments to high specific activity. Anal. Biochem. **137**:266–267.
13. **Feinberg, B., C. S. McLaughlin, and K. Moldave.** 1982. Analysis of temperature-sensitive mutant *ts*187 of *Saccharomyces cerevisiae* altered in a component required for the initiation of protein synthesis. J. Biol. Chem. **257**:10846–10851.
14. **Gross, M., R. Redman, and D. A. Kaplansky.** 1985. Evidence that the primary effect of phosphorylation of eukaryotic initiation factor 2 alpha in rabbit reticulocyte lysate is inhibition of the release of eukaryotic initiation factor-2 · GDP from 60S ribosomal subunits. J. Biol. Chem. **260**:9491–9500.
15. **Gross, M., M. Wing, C. Rundquist, and M. S. Rubino.** 1987. Evidence that phosphorylation of eIF-2(α) prevents the eIF-2B-mediated dissociation of eIF-2 · GDP from the 60S subunit of complete initiation complexes. J. Biol. Chem. **262**:6899–6907.
16. **Hannig, E. H., N. P. Williams, R. C. Wek, and A. G. Hinnebusch.** 1990. The translational activator GCN3 functions downstream from GCN1 and GCN2 in the regulatory pathway that couples GCN4 expression to amino acid availability in *Saccharomyces cerevisiae*. Genetics **126**:549–562.
17. **Hannig, E. M., and A. G. Hinnebusch.** 1988. Molecular analysis of *GCN4*, a translational activator of *GCN4*: evidence for posttranslational control of *GCN3* regulatory function. Mol. Cell. Biol. **8**:4808–4820.
18. **Hansen, L. J., W. Huang, and R. Jagus.** 1987. Inhibitor of translational initiation in sea urchin eggs prevents mRNA utilization. J. Biol. Chem. **262**:6114–6120.
19. **Harashima, S., E. M. Hannig, and A. G. Hinnebusch.** 1987. Interactions between positive and negative regulators of *GCN4* controlling gene expression and entry into the yeast cell cycle. Genetics **117**:409–419.
20. **Harashima, S., and A. G. Hinnebusch.** 1986. Multiple *GCD* genes required for repression of *GCN4*, a transcriptional activator of amino acid biosynthetic genes in *Saccharomyces cerevisiae*. Mol. Cell. Biol. **6**:3990–3998.
21. **Hartwell, L. H., and C. S. McLaughlin.** 1969. A mutant of yeast apparently defective in the initiation of protein synthesis. Proc. Natl. Acad. Sci. USA **62**:468–474.
22. **Helser, T. L., R. A. Baan, and A. E. Dahlberg.** 1981. Characterization of a 40S ribosomal subunit complex in polyribosomes of *Saccharomyces cerevisiae* treated with cycloheximide. Mol. Cell. Biol. **1**:51–57.
23. **Hershey, J. W. B.** 1989. Protein phosphorylation controls translation rates. J. Biol. Chem. **264**:20823–20826.
24. **Hinnebusch, A. G.** 1984. Evidence for translational regulation of the activator of general amino acid control in yeast. Proc. Natl. Acad. Sci. USA **81**:6442–6446.
25. **Hinnebusch, A. G.** 1988. Mechanisms of gene regulation in the general control of amino acid biosynthesis in *Saccharomyces cerevisiae*. Microbiol. Rev. **52**:248–273.
26. **Hoerz, W., and K. S. McCarty.** 1971. Initiation of protein synthesis in a rabbit reticulocyte lysate system. Biochim. Biophys. Acta **228**:526–535.
27. **Ito, H., Y. Fukada, K. Murata, and A. Kimura.** 1983. Transformation of intact yeast cells treated with alkali cations. J. Bacteriol. **153**:163–168.
28. **Kappen, L. S., and I. H. Goldberg.** 1976. Analysis of the two steps in polypeptide chain initiation inhibited by pactamycin. Biochemistry **15**:811–818.
29. **Kappen, L. S., H. Suzuky, and I. H. Goldberg.** 1973. Inhibition of reticulocyte peptide-chain initiation by pactamycin: accumulation of inactive ribosomal initiation complexes. Proc. Natl. Acad. Sci. USA **70**:22–26.
30. **Kleid, D. G., D. Yansura, B. Small, D. Dowbenko, D. M. Moore, M. J. Grubman, P. D. McKercher, D. O. Morgan, B. H. Robertson, and H. L. Bachrach.** 1981. Cloned viral protein vaccine for foot-and-mouth disease: responses in cattle and swine. Science **214**:1125–1129.
31. **Kozak, M., and A. J. Shatkin.** 1978. Migration of 40S ribosomal subunit on messenger RNA in the presence of edeine. J. Biol. Chem. **253**:6568–6577.
32. **Laemmli, U.** 1970. Cleavage of structural proteins during the assembly of the head of bacteriophage T4. Nature (London) **227**:680–685.
33. **Lucchini, G., A. G. Hinnebusch, C. Chen, and G. R. Fink.** 1984. Positive regulatory interactions of the *HIS4* gene of *Saccharomyces cerevisiae*. Mol. Cell. Biol. **4**:1326–1333.
34. **Martin, T. E.** 1973. A simple general method to determine the proportion of active ribosomes in eukaryotic cells. Exp. Cell Res. **80**:496–498.
35. **Martin, T. E., and L. H. Hartwell.** 1970. Resistance of active yeast ribosomes to dissociation by KCl. J. Biol. Chem. **245**:1504–1508.
36. **Moldave, K.** 1985. Eukaryotic protein synthesis. Annu. Rev. Biochem. **54**:1109–1149.
37. **Mueller, P. P., S. Harashima, and A. G. Hinnebusch.** 1987. A segment of *GCN4* mRNA containing the upstream AUG codons confers translational control upon a heterologous yeast transcript. Proc. Natl. Acad. Sci. USA **84**:2863–2867.
38. **Mueller, P. P., and A. G. Hinnebusch.** 1986. Multiple upstream AUG codons mediate translational control of *GCN4*. Cell **45**:201–207.
39. **Niederberger, P., M. Aebi, and R. Huetter.** 1986. Identification and characterization of four new *GCD* genes in *Saccharomyces cerevisiae*. Curr. Genet. **10**:657–664.
40. **Paddon, C. J., E. M. Hannig, and A. G. Hinnebusch.** 1989. Amino acid sequence similarity between GCN3 and GCD2, positive and negative translational regulators of *GCN4*: evidence for antagonism by competition. Genetics **122**:551–559.
41. **Paddon, C. J., and A. G. Hinnebusch.** 1989. *gcd12* mutations are *gcn3*-dependent alleles of *GCD2*, a negative regulator of *GCN4* in the general amino acid control of *Saccharomyces cerevisiae*. Genetics **122**:543–550.
42. **Palmer, E., J. Wilhelm, and F. Sherman.** 1979. Phenotypic

suppression of nonsense mutants in yeast by aminoglycoside antibiotics. Nature (London) **277**:148–150.
43. **Peterson, D. T., B. Safer, and W. C. Merrick.** 1979. Role of eukaryotic initiation factor 5 in the formation of 80S initiation complexes. J. Biol. Chem. **254**:7730–7735.
44. **Petes, T. D., L. M. Hereford, and K. G. Skryabin.** 1978. Characterization of two types of yeast ribosomal DNA genes. J. Bacteriol. **134**:295–305.
45. **Raychaudhuri, P., E. A. Stringer, D. M. Valenzuela, and U. Maitra.** 1984. Ribosomal subunit antiassociation activity in rabbit reticulocyte lysates. J. Biol. Chem. **259**:11930–11935.
46. **Rhoads, R. E.** 1988. Cap recognition and the entry of mRNA into the protein synthesis initiation cycle. Trends Biochem. Sci. **13**:52–56.
47. **Rotenberg, M. O., M. Moritz, and J. L. Woolford, Jr.** 1988. Depletion of *Saccharomyces cerevisiae* ribosomal protein L16 causes a decrease in 60S ribosomal subunits and formation of half-mer polyribosomes. Genes Dev. **2**:160–172.
48. **Sonenberg, N.** 1990. Measures and countermeasures in the modulation of initiation factor activities by viruses. New Biol. **2**:402–409.
49. **Struhl, K., D. T. Stinchomb, S. Scherer, and R. W. Davis.** 1979. High frequency transformation of yeast: autonomous replication of hybrid DNA molecules. Proc. Natl. Acad. Sci. USA **76**:1035–1039.
50. **Szczesna, E., and W. Filipowicz.** 1980. Faithful and efficient translation of viral and cellular eukaryotic mRNAs in a cell-free S-27 extract of *Saccharomyces cerevisiae*. Biochem. Biophys. Res. Commun. **92**:563–569.
51. **Towbin, H., T. Staehelin, and J. Gordon.** 1979. Electrophoretic transfer of proteins from polyacrylamide gels to nitrocellulose: procedure and some applications. Proc. Natl. Acad. Sci. USA **83**:4849–4853.
52. **Tzamarias, D., I. Roussou, and G. Thireos.** 1989. Coupling of GCN4 mRNA translational activation with decreased rates of polypeptide chain initiation. Cell **57**:947–954.
53. **Van Venrooij, W. J., J. Van Eenbergen, and A. P. M. Janssen.** 1977. Effect of anisomycin on the cellular level of native ribosomal subunits. Biochemistry **16**:2343–2348.
54. **Williams, N. P., A. G. Hinnebusch, and T. F. Donahue.** 1989. Mutations in the structural genes for eukaryotic initiation factors 2alpha and 2beta of *Saccharomyces cerevisiae* disrupt translational control of *GCN4* mRNA. Proc. Natl. Acad. Sci. USA **86**:7515–7519.
55. **Wolfner, M., D. Yep, F. Messenguy, and G. R. Fink.** 1975. Integration of amino acid biosynthesis into the cell cycle of *Saccharomyces cerevisiae*. J. Mol. Biol. **96**:273–290.